

Femtosecond laser induced synthesis of Au nanoparticles mediated by chitosan

P. H. D. Ferreira, M. G. Vivas, L. De Boni, D. S. dos Santos Jr., D. T. Balogh, L. Misoguti and C. R. Mendonca*

Instituto de Física de São Carlos, Universidade de São Paulo, Caixa Postal 369, 13560-970 São Carlos, Sao Paulo, Brazil

*crmendon@if.sc.usp.br

Abstract: This paper reports the synthesis of Au nanoparticles by 30-fs pulses irradiation of a sample containing H₂AuCl₄ and chitosan, a biopolymer used as reducing agent and stabilizer. We observed that it is a multi-photon induced process, with a threshold irradiance of 3.8×10^{11} W/cm² at 790 nm. By transmission electron microscopy we observed nanoparticles from 8 to 50 nm with distinct shapes. Infrared spectroscopy indicated that the reduction of gold and consequent production of nanoparticles is related to the fs-pulse induced oxidation of hydroxyl to carbonyl groups in chitosan.

© 2011 Optical Society of America

OCIS codes: (160.4236) Nanomaterials; (190.0190) Nonlinear optics; (320.2250) Femtosecond phenomena.

References and links

1. A. N. Shipway, E. Katz, and I. Willner, "Nanoparticle arrays on surfaces for electronic, optical, and sensor applications," *ChemPhysChem* **1**(1), 18–52 (2000).
2. M. C. Daniel and D. Astruc, "Gold nanoparticles: assembly, supramolecular chemistry, quantum-size-related properties, and applications toward biology, catalysis, and nanotechnology," *Chem. Rev.* **104**(1), 293–346 (2004).
3. Y. C. Cao, R. C. Jin, and C. A. Mirkin, "Nanoparticles with Raman spectroscopic fingerprints for DNA and RNA detection," *Science* **297**(5586), 1536–1540 (2002).
4. M. Moskovits, "Surface-Enhanced Spectroscopy," *Rev. Mod. Phys.* **57**(3), 783–826 (1985).
5. S. Eustis and M. A. el-Sayed, "Why gold nanoparticles are more precious than pretty gold: noble metal surface plasmon resonance and its enhancement of the radiative and nonradiative properties of nanocrystals of different shapes," *Chem. Soc. Rev.* **35**(3), 209–217 (2006).
6. G. Frens, "Controlled Nucleation for Regulation of Particle-Size in Monodisperse Gold Suspensions," *Nature* **241**, 20–22 (1973).
7. S. D. Bunge, T. J. Boyle, and T. J. Headley, "Synthesis of coinage-metal nanoparticles from mesityl precursors," *Nano Lett.* **3**(7), 901–905 (2003).
8. M. Sakamoto, M. Fujistuka, and T. Majima, "Light as a construction tool of metal nanoparticles: Synthesis and mechanism," *J. Photochem. Photobiol. Photochem. Rev.* **10**(1), 33–56 (2009).
9. T. Hassenkam, K. Norgaard, L. Iversen, C. J. Kiely, M. Brust, and T. Bjornholm, "Fabrication of 2D gold nanowires by self-assembly of gold nanoparticles on water surfaces in the presence of surfactants," *Adv. Mater. (Deerfield Beach Fla.)* **14**(16), 1126–1130 (2002).
10. S. S. Shankar, A. Rai, B. Ankamwar, A. Singh, A. Ahmad, and M. Sastry, "Biological synthesis of triangular gold nanoprisms," *Nat. Mater.* **3**(7), 482–488 (2004).
11. S. P. Chandran, M. Chaudhary, R. Pasricha, A. Ahmad, and M. Sastry, "Synthesis of gold nanotriangles and silver nanoparticles using Aloe vera plant extract," *Biotechnol. Prog.* **22**(2), 577–583 (2006).
12. I. Willner, R. Baron, and B. Willner, "Growing metal nanoparticles by enzymes," *Adv. Mater. (Deerfield Beach Fla.)* **18**(9), 1109–1120 (2006).
13. H. Z. Huang and X. R. Yang, "Synthesis of chitosan-stabilized gold nanoparticles in the absence/presence of triphosphosphate," *Biomacromolecules* **5**(6), 2340–2346 (2004).
14. D. S. dos Santos, Jr., P. J. G. Goulet, N. P. W. Pieczonka, O. N. Oliveira, Jr., and R. F. Aroca, "Gold nanoparticle embedded, self-sustained chitosan films as substrates for surface-enhanced Raman scattering," *Langmuir* **20**(23), 10273–10277 (2004).
15. D. W. Wei and W. P. Qian, "Facile synthesis of Ag and Au nanoparticles utilizing chitosan as a mediator agent," *Colloids Surf. B Biointerfaces* **62**(1), 136–142 (2008).

16. D. W. Wei and W. P. Qian, "Chitosan-mediated synthesis of gold nanoparticles by UV photoactivation and their characterization," *J. Nanosci. Nanotechnol.* **6**(8), 2508–2514 (2006).
 17. W. A. Bough, W. L. Salter, A. C. M. Wu, and B. E. Perkins, "Influence of Manufacturing Variables on Characteristics and Effectiveness of Chitosan Products. 1. Chemical Composition, Viscosity, and Molecular-Weight Distribution of Chitosan Products," *Biotechnol. Bioeng.* **20**(12), 1931–1943 (1978).
 18. J. Turkevich, P. C. Stevenson, and J. Hillier, "A Study of the Nucleation and Growth Processes in the Synthesis of Colloidal Gold," *Discuss. Faraday Soc.* 55-75 (1951).
 19. M. Sheik-Bahae, A. A. Said, T. H. Wei, D. J. Hagan, and E. W. Van Stryland, "Sensitive Measurement of Optical Nonlinearities Using a Single Beam," *IEEE J. Quantum Electron.* **26**(4), 760–769 (1990).
 20. A. Vogel, J. Noack, K. Nahen, D. Theisen, S. Busch, U. Parltitz, D. X. Hammer, G. D. Noojin, B. A. Rockwell, and R. Birngruber, "Energy balance of optical breakdown in water at nanosecond to femtosecond time scales," *Appl. Phys. B* **68**(2), 271–280 (1999).
 21. J. Noack, D. X. Hammer, G. D. Noojin, B. A. Rockwell, and A. Vogel, "Influence of pulse duration on mechanical effects after laser-induced breakdown in water," *J. Appl. Phys.* **83**(12), 7488–7495 (1998).
 22. C. F. Bohren and D. R. Huffman, *Absorption and Scattering of Light by Small Particles* (Wiley, 1983).
 23. J. Grant, M. Blicher, M. Piquette-Miller, and C. Allen, "Hybrid films from blends of chitosan and egg phosphatidylcholine for localized delivery of paclitaxel," *J. Pharm. Sci.* **94**(7), 1512–1527 (2005).
 24. J. Grant, J. Cho, and C. Allen, "Self-assembly and physicochemical and rheological properties of a polysaccharide-surfactant system formed from the cationic biopolymer chitosan and nonionic sorbitan esters," *Langmuir* **22**(9), 4327–4335 (2006).
-

1. Introduction

Research on synthesis, fabrication and processing of nanostructured materials has received a great deal of attention because of their potential applications in fundamental science and nanotechnology [1–5]. Several methods to produce metal nanoparticles, including chemical, photochemical and thermal have been developed to allow controlling size and shape of nanostructures [2, 6–9]. More recently, however, biomolecules and live organisms have also been utilized for the synthesis of Ag and Au nanoparticles [10–12]. The interest in such biosynthetic approach has been motivated because it can be easily controlled under mild conditions and does not introduce environmental toxicity or biological hazards [13–15]. At the same time, photochemical methods using *cw* irradiation of a solution containing metal ions with ultra-violet or blue light [13–15] has also been exploited as an interesting option to produce metal nanoparticles. Conversely, such type of irradiation can lead to undesirable photochemical reactions, which ultimately could change a desired property of the final product, affecting, for instance, the stabilizer that encapsulates the nanoparticles.

To overcome this potential drawback, in this paper we demonstrate the use of infrared fs-laser pulses to produce nanoparticles in a sample containing HAuCl₄ and the biopolymer chitosan. Therefore, the method proposed here combines the advantage of a biosynthetic approach with the innovative and still unexplored use of infrared fs-pulses for the synthesis of nanoparticles. Chitosan was chosen because it is one of the most studied bio-macromolecules for the production nanoparticles. Moreover, it has been shown to act as a reducing agent and stabilizer in the nanoparticles synthesis (chemical or photochemical) [13–16]. In this study, the excitation was performed with 30-fs pulses at 790 nm, operating in the transparent region of the sample. Our results show that the production of Au nanoparticles is related to the multi-photon induced oxidation of chitosan and subsequent reduction of Au. The ability to synthesize Au nanoparticles by such nonlinear optical interaction opens new possibilities in this area, such as using pulse shaping methods to achieve control of the photochemical reaction.

2. Experimental

The production of Au nanoparticles was carried out employing chitosan as the stabilizer and reducing agent in the photoreduction of tetrachloroauric acid (HAuCl₄) induced by femtosecond pulses at 790 nm. Chitosan [(1→4)-2 amino -2 -deoxy-β-D-glucan] is a linear cationic polysaccharide obtained by deacetylation of chitin [(1→4)-2 acetamide -2 -deoxy-β-D-glucan], which is normally found in crustaceans. However, it is not completely

deacetylated, being therefore a copolymer of acetamide and amine groups. Chitosan was extracted from gray shrimps chitin using the method described in Ref [17], and purified by dissolution in acetic acid, precipitated in NH_4OH and filtered using a $45\ \mu\text{m}$ membrane. It has a molecular weight (Mw) of $8 \times 10^4\ \text{g/mol}$, determined by viscometry [17], and a degree of acetylation (DA) of 14, determined by proton NMR using deuterated water. The molecular structure of chitosan is presented in the detail of Fig. 1.

The tetrachloroauric acid (HAuCl_4) solution and acetic acid were purchased from Aldrich and used without further purification. A solution of chitosan in acetic acid (0.24 wt%) was prepared by adding 2 mL of glacial acetic acid to 0.1 g of chitosan and then diluting with 40 mL of ultrapure water while stirring. The aqueous solution of HAuCl_4 (0.2 wt%) was mixed with the chitosan solution in a 1:3 volume ratio at room temperature, which corresponds to an equimolar proportion of chitosan repeating units to Au. The sample was placed in a 2-mm path-length quartz cuvette for linear and nonlinear optical experiments.

As the excitation source for the photo-reduction, we used 30-fs pulses from a multi-pass amplifier (790 nm and 1 kHz repetition rate). To monitor the dynamics of Au nanoparticles formation, we measured the time evolution of the plasmon absorption band using a pump-probe scheme, as illustrated in Fig. 1. The sample is excited by a laser beam with a diameter of 1.6-mm and irradiances varying from $4 \times 10^{11}\ \text{W/cm}^2$ to $14 \times 10^{11}\ \text{W/cm}^2$. The time-evolution of the sample absorption was determined using a white LED (430–600 nm) as a probe beam, whose light was measured by a spectrometer. The probe beam does not produce any excitation of the sample. The sample is automatically agitated (5 Hz), perpendicularly to the pump and probe beams, throughout the entire experiment to homogenize the distribution of the produced Au nanoparticles.

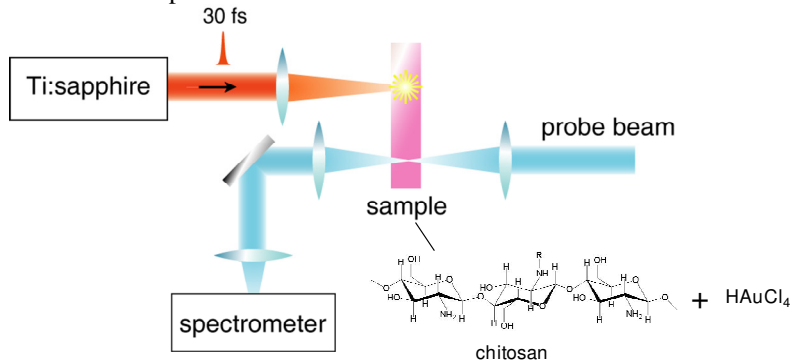


Fig. 1. Experimental setup used to measure the plasmon band during the nanoparticles formation. In the detail, we display the molecular structure of chitosan.

UV-Vis spectra of the samples were measured with a Cary-17 spectrometer at room temperature. Transmission electron microscopy (TEM) images were obtained with a Philips CM120 scanning electron transmission microscope. The solutions used in the irradiation experiments were casted onto silicon windows and dried in vacuum at room temperature overnight to perform infrared absorption experiments. Infrared absorption spectra of these samples were recorded in a ThermoNicolet Nexus 470 Fourier transform infrared (FTIR) spectrometer in transmission mode, with 32 scans and $4\ \text{cm}^{-1}$ resolution.

3. Results and discussion

Using chitosan as the stabilizer and reducing agent, the production of gold nanoparticles, promoted by the excitation with fs-pulses, is illustrated in Fig. 2. As can be seen, after 2 hours of irradiation with a pulse intensity of $6.8 \times 10^{11}\ \text{W/cm}^2$, the spectrum exhibit absorption centered at approximately 535 nm (black line), which is the characteristic plasmon resonance band for gold nanoparticles, indicating, therefore, the formation of gold nanoparticles [13, 16, 18]. In Fig. 2 (a), the gray line shows the UV-Vis absorption of the

sample before the fs-pulse irradiation, showing that it is completely transparent for wavelengths higher than 550 nm. Visually we observe a change in the color of the solution from light yellow to pink as the reaction proceeds. In supplementary experiments, we observed that no color change takes place if chitosan is not present in the sample being irradiated. It is important to note that the sample, either before or after irradiation, is completely transparent in the near infrared region, where the fs-pulse excitation is carried out (790 nm). Hence, the fs-induced reduction of gold is driven by a nonlinear optical process. Since ultra-violet light has been shown to produce nanoparticles in the presence of Au ions and chitosan (linear optical process) [13–15], the first hypothesis to explain our results would be a two-photon excitation of a state located around 395 nm (two photons of 790 nm), in a process analogous to the linear optical one [13–15]. However, open aperture Z-scan measurements [19] in a chitosan sample, carried out around 790 nm, showed no results, indicating that there is no two-photon state at this wavelength or its two-photon absorption cross-section is negligible, ruling out this hypothesis. Therefore, nonlinear ionization of chitosan could be a possible mechanism responsible for the reduction of the gold, and subsequent formation of nanoparticles as will be discussed later.

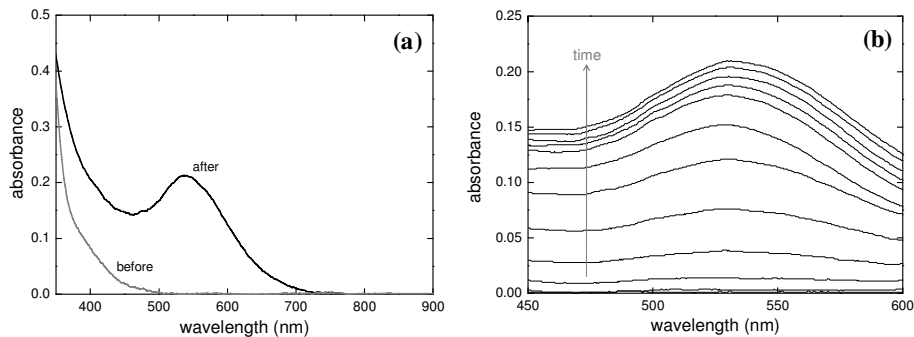


Fig. 2. (a) UV-Vis absorption spectra of the solution containing HAuCl_4 and chitosan before and after the fs-laser irradiation ($6.8 \times 10^{11} \text{ W/cm}^2$ and 2 hours). (b) Growth of the surface plasmon absorption band with the reaction time, indicating the production of gold nanoparticles ($6.8 \times 10^{11} \text{ W/cm}^2$). Each curve was obtained at 10 minutes intervals. The last curve corresponds to 120 minutes, when the process was stopped.

In Fig. 2 (b), we present the time evolution of the plasmon band during irradiation ($6.8 \times 10^{11} \text{ W/cm}^2$), measured with the pump-probe setup described previously. The spectra in Fig. 2 (b) were collected at time intervals of 10 minutes, with the last curve obtained at 120 minutes. The evolution of the plasmon band around 535 nm with reaction time is attributed to nucleation, growth and increasing amount of gold nanoparticles in the sample.

In order to examine the dependence of the gold nanoparticles formation with the irradiation, we normalized the curves in such a way that the last one (at 120 minutes) has a peak intensity of one. In Fig. 3, we plot the normalized absorbance at 535 nm as a function of time for three distinct laser irradiances. While for an intensity of $4.6 \times 10^{11} \text{ W/cm}^2$ the plasmon band appears only after about 60 minutes, the nanoparticles formation process is much faster for the pulse irradiance of $7.0 \times 10^{11} \text{ W/cm}^2$. In this last case, the plasmon band starts to rise after 20 minutes. It is worth mentioning that we were only able to observe nanoparticles formation for pulse irradiances higher than $3.8 \times 10^{11} \text{ W/cm}^2$. By plotting the plasmon band magnitude at 80 minutes as a function of the femtosecond laser irradiance (results not shown), a slope of approximately four was observed, indicating a multi-photon induced ionization process. Such time was chosen because at it all curves are in approximately the same regime of the nanoparticles production process (see Fig. 3), i.e., the growth of the plasmon band is not close to saturation (which starts to occur at ~ 100 minutes) nor the plasmon absorption is too small to be properly determined. In the irradiance range used ($4 \times 10^{11} \text{ W/cm}^2$ to $14 \times 10^{11} \text{ W/cm}^2$), optical breakdown was not observed, which is

consistent with the breakdown threshold experimentally observed for water (approximately $100 \times 10^{11} \text{ W/cm}^2$ for 100 fs pulses) [20, 21]. Furthermore, to avoid white-light continuum generation, we employed an excitation beam diameter of 1.6 mm and a 2-mm path-length cuvette, preventing self-focusing.

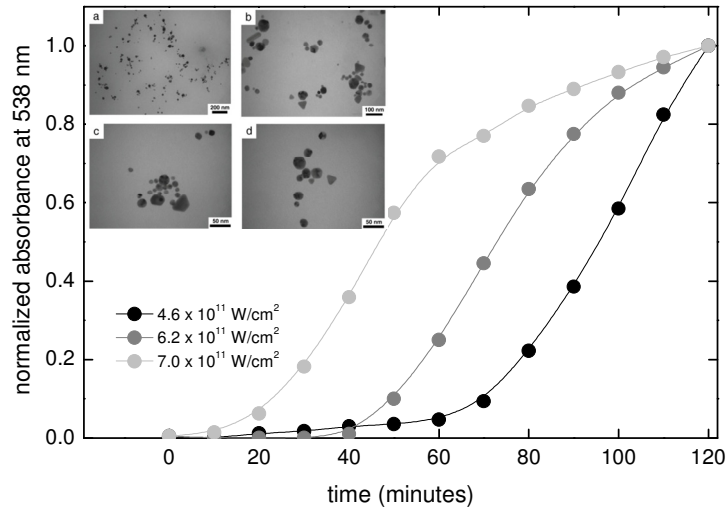


Fig. 3. Normalized absorption at 535 nm as a function of time during the fs-laser irradiation for distinct pulse intensities. The inset shows TEM images of the nanoparticles synthesized by fs-laser irradiation.

The UV-Vis absorption curves presented in Fig. 2 (b) suggested the synthesis of gold nanoparticles induced by fs-laser excitation. Such result was further confirmed by TEM measurements. TEM images of gold nanoparticles reduced/stabilized by chitosan upon fs-laser irradiation are displayed in inset of Fig. 3. In general, particles are mostly spherical in shape, although other shapes such as rods and prisms are also observed. As can be seen in inset of Fig. 3, nanoparticles with a wide size distribution are obtained, which is in agreement with the broad absorption band observed (Fig. 2). Such distribution can be attributed to the slow reduction process induced by multi-photon absorption. It is noteworthy that we did not observe any dependence of the shape or size of the produced Au nanoparticles with the laser intensity or exposure time.

By using Mie theory [22], considering separated spheres embedded in a medium with a refractive index of 1.5, an absorption peak is obtained at 535 nm (peak position experimentally observed) for nanoparticles with 20 nm of diameter. Such estimated value is in reasonable agreement with the size distribution observed in the TEM images (inset of Fig. 3), since the produced nanoparticles are in the size range from 8 nm to 50 nm.

To explore the fs-laser induced reduction process of gold with chitosan, FTIR measurement were carried out to study possible interactions and redox process which resulted in the generation of nanoparticles. All the characteristic absorption bands could be clearly observed in the FTIR spectrum of chitosan: a broad band of OH stretchings at $3500\text{-}3100 \text{ cm}^{-1}$; a peak of NH stretching at around 3300 cm^{-1} partially overlapped by the OH stretching, aliphatic CH stretchings at around $2920, 2870 \text{ cm}^{-1}$; C-N stretching at 1310 cm^{-1} and absorptions of NH_3^+ associated with acetate groups at 1560 cm^{-1} , since this spectrum was obtained from a thin film prepared with chitosan dissolved in acetic acid solution.

Figure 4 presents FTIR spectra in the region of $1800 \text{ to } 1200 \text{ cm}^{-1}$ (finger print) of the films made from the pristine chitosan solution (a), gold chloride/chitosan solution (b) and the irradiated gold nanoparticle/chitosan solution (c) (obtained by fs-laser irradiation with $140 \mu\text{J}$ for 2 hours). The rest of the spectra are not shown because there are no significant differences. No differences between the spectra obtained with chitosan solution before and

after irradiation could be observed, therefore, the spectrum of the later is not shown. Interactions between the gold chloride and NH groups of chitosan can be inferred by the changes observed in the 1650-1300 cm^{-1} region, comparing the spectra of chitosan and chitosan/gold chloride prior to the irradiation. The band at around 1560 cm^{-1} shifted to 1520 cm^{-1} indicates that the acetate counter ions were replaced by the AuCl_4^- , and the decreasing of the intensity of the absorption at around 1406 cm^{-1} corroborate this displacement. After irradiation, the increase in the intensity of the absorption at around 1620 cm^{-1} , characteristic of NH_2 (or CONH_2), indicates the release of some AuCl_4^- counter-ions [23, 24]. The appearance of the band around 1730 cm^{-1} in the gold/chitosan irradiated sample, characteristic of aldehyde groups, indicates that the reduction of the gold ions for the formation of the gold nanoparticles is related to the oxidation of hydroxyl groups in chitosan to carbonyl groups [15, 16]. This result agrees with our hypothesis that the production of Au nanoparticles is probably related to the ionization (oxidation) of the chitosan induced by fs-laser pulses.

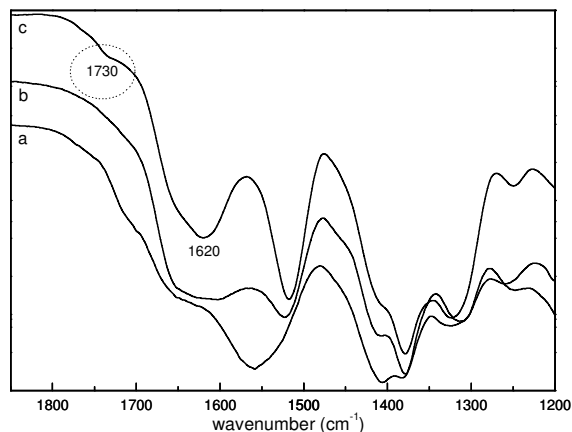


Fig. 4. FTIR spectra in the finger print region of pristine chitosan (a), chitosan/gold chloride (b) and irradiated chitosan/gold chloride (c).

4. Conclusions

We have demonstrated the production of gold nanoparticles in an aqueous solution containing tetrachloroauric acid (HAuCl_4) and the biopolymer chitosan, upon excitation with 30-fs pulses at 800 nm. The synthesis of the nanoparticles was monitored by the plasmon resonance band, while the shapes (spheres, rods and prisms) and dimensions (8-50 nm) of the nanoparticles were determined by transmission electron microscopy. Our results indicate that fs-pulses induce the oxidation of hydroxyl to carbonyl groups in chitosan, leading, subsequently, to the reduction of gold ions and consequent production of nanoparticles. Therefore, the approach presented here can open new ways to produce metallic nanoparticles in solution, for instance, by applying fs-pulse shaping methods to control the process. Furthermore, such approach could be employed with other stabilizers or reducing agents.

Acknowledgments

This work was supported by Fundação de Amparo à Pesquisa do Estado de São Paulo (FAPESP), Conselho Nacional de Desenvolvimento Científico e Tecnológico (CNPq) and Coordenação de Aperfeiçoamento de Pessoal de Nível Superior (CAPES).